**Title**
Range Dependence of the HRTF for a Spherical Head



**Authors**
Duda, Richard O
Martens, W. L.

**Publication Date**
1997

Peer reviewed

# RANGE-DEPENDENCE OF THE HRTF FOR A SPHERICAL HEAD

*Richard O. Duda*

Department of Electrical Engineering
San Jose State University
San Jose, CA 95192
email: rod@duda.org

*William L. Martens*

Human Interface Lab
University of Aizu
Aizu-Wakamatsu 965-80 Japan
email: wlm@u-aizu.ac.jp

## ABSTRACT

This paper examines the range dependence of the HRTF for a simple spherical model of the head in both the time-domain and the frequency domain. The variation of low-frequency ILD with range is shown to be significant for ranges smaller than five times the sphere radius. The impulse response explains the source of the ripples in the frequency response, and provides direct evidence that the Interaural Time Delay (ITD) is not a strong function of range. Time-delay measurements confirm the Woodworth/Schlosberg formula. Numerical analysis indicates that the HRTF is minimum phase. Thus, except for time delay, the impulse response can be reconstructed from a simple principle components analysis of the magnitude response.

## 1. INTRODUCTION

The human Head-Related Transfer Function (HRTF) varies with range as well as with azimuth and elevation. In particular, the low-frequency Interaural Level Difference (ILD), which is negligible at large distances, becomes large at close distances. This paper, which extends earlier work by Brungart and Rabinowitz [1], focuses on the range dependence of the sound pressure on an ideal rigid sphere due to a point source. Our purpose is to obtain a better understanding of the behavior of the head-related transfer function (HRTF) at close ranges.

It is common experience that sounds from a source that is very close to one's ear are not only louder but also contain more low-frequency energy than sounds from a distant source. The simplest model that explains these effects approximates the source by a point source and approximates the head by a rigid sphere. While this idealization is restricted to relatively low frequencies and obviously becomes problematic very close to the surface of the head, a quantitative understanding of its behavior provides insight into the more complex behavior of the HRTF for an actual human head and a distributed source.

We present both theoretical and experimental results. We examine the behavior of the theoretical solution in both the frequency domain (the HRTF) and the time domain (the head-related impulse response, or HRIR). The time-domain solution provides insight into some otherwise puzzling behavior of the HRTF.

## 2. FREQUENCY-DOMAIN SOLUTION

Rabinowitz et al. [2] present a formula for the pressure on the surface of the sphere due to a sinusoidal point source at any range $r$ greater than the sphere radius $a$. Their solution is expressed in the frequency domain as an infinite series for the HRTF $H(\rho,\mu,\theta)$, the ratio of the phasor pressure at the surface of the sphere to the phasor free-field pressure at the center of the sphere. Here $\rho = r / a$ is the normalized range, $\mu = \omega\, a / c$ is the normalized frequency ($\omega$ is the angular frequency and $c$ is the speed of sound), and $\theta$ is the angle of incidence — the angle between a ray from the center of the sphere to the sound source and a ray from the center of the sphere to the observation point.

We used the infinite series given in [2] to compute both the HRTF and the HRIR. The magnitude of the HRTF for a source at infinity is shown in Fig. 1. This classical result shows that the pressure on the sphere is the same as the free-field pressure at low frequencies. For normal incidence ($\theta = 0°$), the pressure increases with frequency, rising about 6 dB at high frequencies. The critical frequency $\mu = 1$ corresponds to 624 Hz for the traditional "average head radius" of 8.75 cm. The magnitude response is roughly flat when $\theta = 100°$, and falls off in a rather complicated fashion for larger $\theta$. Near the back of the sphere, the response exhibits large ripples, and rises to a "bright spot" at the contralateral point.

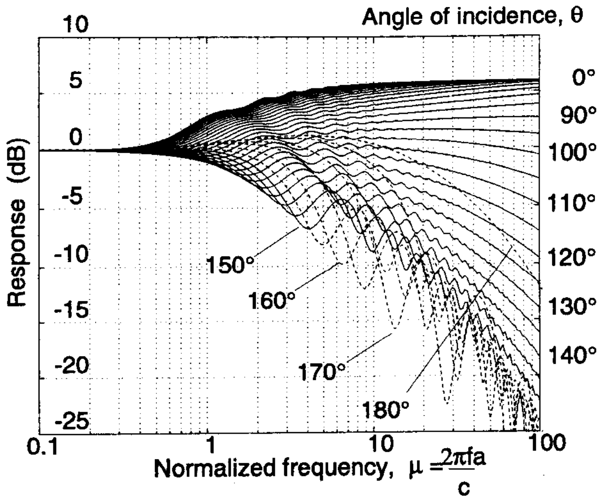


**Figure 1:** Magnitude response for a source at infinity

Brungart and Rabinowitz [1] assumed that the ears were at opposite ends of a diameter, and computed how the ILD and ITD vary with range. Following Blauert [3], we placed the ears back an additional 10° and computed the ILD surfaces shown in Figs. 2-4. The ILD in Fig. 2 for $\rho = 100$ is less than 3 dB for $\mu < 1$. This begins to change significantly when $\rho$ is less than 5. For example, the low-frequency ILD for $\rho = 2$ can exceed 10 dB (Fig. 3), and can exceed 20 dB for $\rho = 1.25$ (Fig. 4).

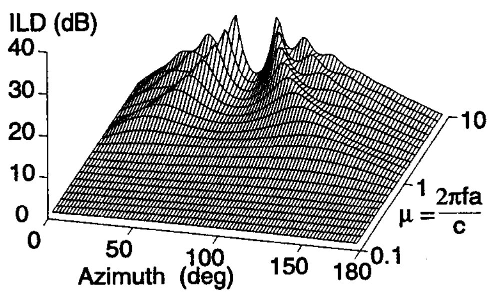


**Figure 2:** ILD for $\rho = 100$ and the ears at ±100°

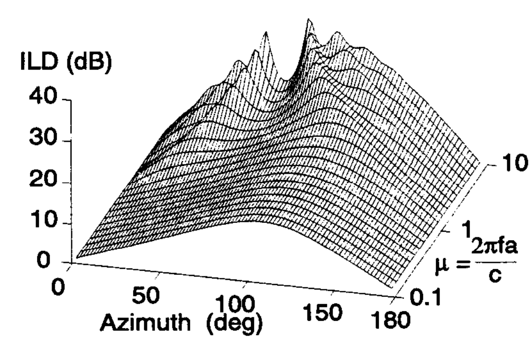


**Figure 3:** ILD for $\rho = 2$

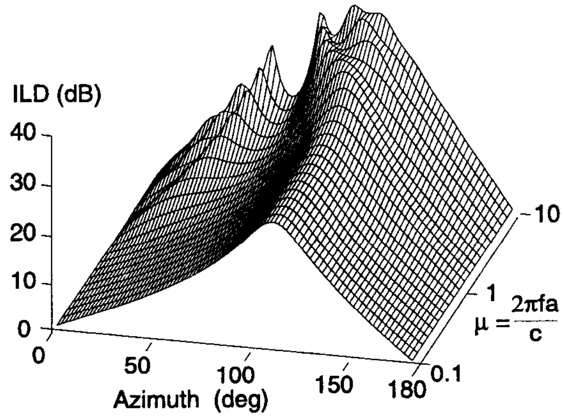


**Figure 4:** ILD for $\rho = 1.25$

## 3. IMPULSE RESPONSE

As we explain ahead, there is good evidence that the HRTF for a sphere is minimum-phase, so that the HRIR can be recovered from the magnitude response. It can also be obtained directly by inverse Fourier transforming the transfer function,

$$h(\rho, \tau, \theta) = \int_{-\infty}^{\infty} H(\rho, \mu, \theta)\, e^{-i2\pi\mu\tau}\, d\mu \quad ,$$

where $\tau$ is the normalized time given by $\tau = c\,t / 2\,\pi\,a$ . Fig. 5 shows the results of evaluating the transform numerically for the case $\rho = 100$. Note that as the angle of incidence $\theta$ approaches 180°, the bright spot becomes prominent in the HRIR. Moreover, the visual appearance of the graph strongly suggests that the impulse "ridge" continues on through the bright spot.

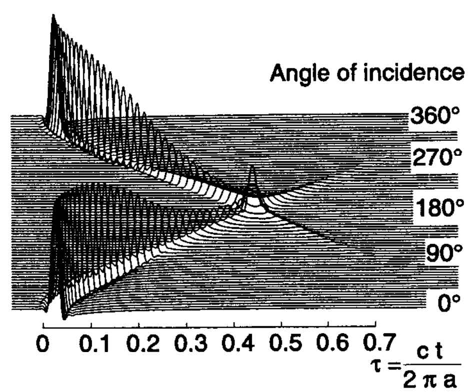


**Figure 5:** The HRIR for $\rho = 100$

One can interpret the overall response as being the result of two waves — one propagating around the right side of the sphere, and the other propagating around the left side, with the bright spot emerging where these two waves meet. Although this is a very rough approximation, it explains why the responses for incidence angles between about 150° and 170° contain two prominent pulses in the time domain, and it also explains the emergence of a corresponding strong pattern of ripples in the frequency domain.

Fig. 6 shows the HRIR for ρ = 1.25. As the source is brought closer to the sphere, the response becomes stronger on the near side and weaker and broader on the far side. In addition, the difference between the time of arrival at the near side and at the far side is somewhat smaller at long ranges (Fig. 5) than at close ranges (Fig. 6).

When we used the MATLAB™ rceps function to compute minimum-phase reconstructions of the impulse responses in Figs. 5 and 6, the only significant change was the expected time shift. While we do not have a mathematical proof, we believe that this is strong evidence that the impulse response of the sphere is minimum phase.

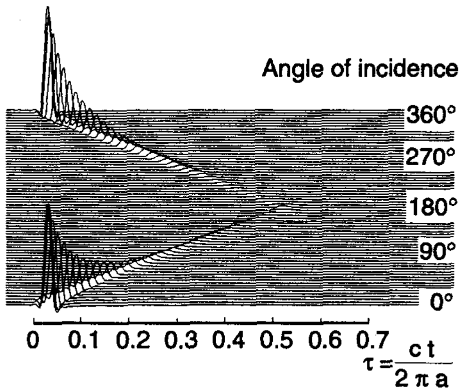


**Figure 6:** The HRIR; range is 1.25 times the sphere radius

## 4. TIME DELAY

With transfer functions, it is common to use the phase and/or group delays to define the arrival time of a pulse. The phase delay for the sphere is frequency dependent, being 50% greater at low frequencies than at high frequencies [4]. With experimentally measured data, it is convenient to define the arrival time by $\Delta t_p$, the time at which the pulse first exceeds $p$ times its maximum amplitude. We used this same definition is used to compute the normalized arrival time for the computed HRIR, so that $\Delta\tau_p = c\,\Delta t_p / 2\pi a$, with $p$=0.15.

The open circles in Fig. 7 show how this normalized arrival time varies with the angle of incidence for two different normalized ranges, ρ = 1.25 and ρ = 100. These two curves bound the results at intermediate ranges. Since Δτ is the (normalized) difference between the time of arrival at the surface of the sphere and the free-field time of arrival at the center of the sphere, when θ = 0, Δτ is negative for all ranges. At larger azimuths, Δτ becomes larger as the source approaches the sphere. In addition, the interaural time differ-ence (ITD), which is given by Δτ(θ+100°) - Δτ(θ-100°), also becomes larger as the source approaches the sphere.

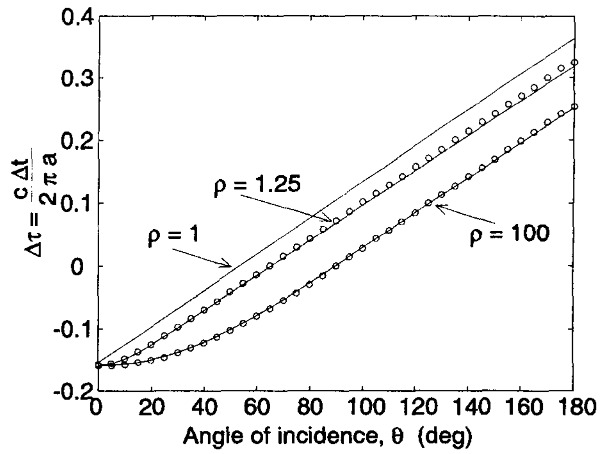


**Figure 7:** Normalized arrival time for three different ranges

A formula due to Woodworth and Schlosberg can be generalized to provide useful approximate equations for the time delay and ITD [3]. The normalized time difference Δτ between the time that the wave reaches the observation point and the time that it would reach the center of the sphere in free field is given by

$$\Delta\tau = \begin{cases} \frac{1}{2\pi}\left(\sqrt{\rho^2 - 2\rho\cos\theta + 1} - \rho\right) & \text{if } 0 \le \theta \le \theta_0 \\ \frac{1}{2\pi}\left(\theta - \theta_0 + \sqrt{\rho^2 - 1} - \rho\right) & \text{if } \theta_0 \le \theta \le \pi \end{cases}, \quad (1)$$

where

$$\theta_0 = \cos^{-1}(1/\rho) \quad , \rho \ge 1. \quad (2)$$

The solid-line curves in Fig. 7 show the predictions of this simple model for ρ = 1, 1.25, and ∞, and are within 2.4% of the 15%-rise-time results.

Finally, Fig. 8 shows bounds on the ITD computed from (1) and (2) for ears located at θ = ±100°. Bringing the source closer to the sphere increases the ITD as much as 25.7% (0.0908 normalized units, or 146 μs for an 8.75-cm head radius). Brungart and Rabinowitz (1996) obtained similar results using the phase delay. They pointed out that humans are insensitive to time delays above 700 μs, and the results shown here support their conjecture that changes in the ITD probably do not provide significant information about range.

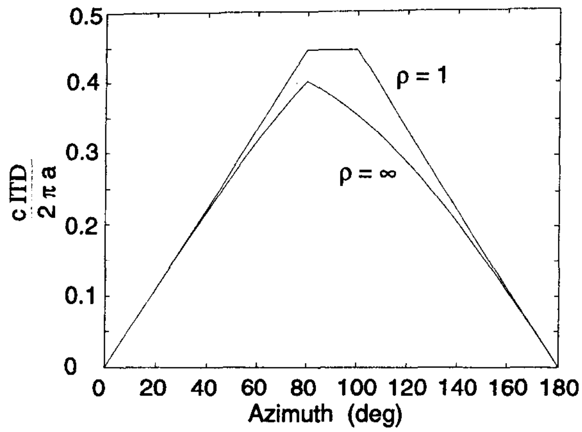


**Figure 8:** Upper and lower bounds on the normalized ITD

## 5. EXPERIMENTAL MEASUREMENTS

We have been using the Crystal River Engineering Snapshot™ system to measure HRIR's for human subjects. As an experiment, we decided to use this system to repeat Wiener's measurements of a sphere [5]. An Etymotic Research ER-7C probe microphone was inserted in a hole drilled through an 3.6-kg, 10.9-cm radius bowling ball (for which $\mu = 1$ corresponds to 500 Hz). The ball was mounted on a 1.3-cm diameter vertical rod which supported it 1 m from the floor of the anechoic chamber. Measurements were made for $\rho$ = 1.25, 1.5, 2, 3, 5, 10 and 20. To reduce perceptually irrelevant fine structure, the squared magnitude of the free-field compensated HRTF was smoothed with a 10% bandwidth auditory filter.

An example of the resulting frequency response curves is shown in Fig. 9. For comparison, the solid lines show the smoothed theoretical results. Similar results were obtained at other angles and ranges, although significant discrepancies began to appear when $\rho < 2$ and the source could no longer be approximated well by a point source. Fig. 10 shows the corresponding HRIR. Again, the results are remarkably similar to the theoretical predictions (c.f. Fig. 5).

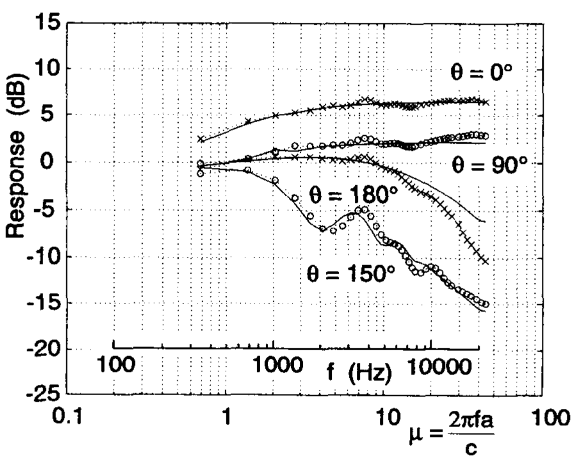


**Figure 9:** Measured and theoretical HRTF magnitudes, $\rho = 20$

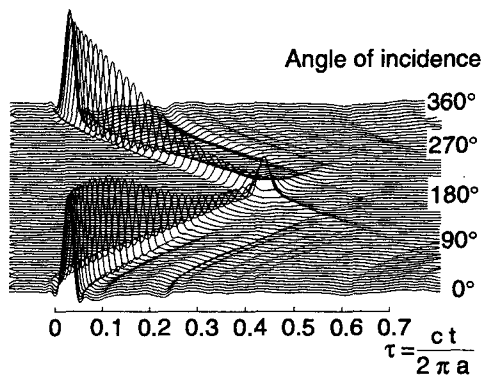


**Figure 10:** Measured impulse response, $\rho = 20$

Finally, Fig. 11 shows the time delay computed from the experimentally measured HRIR's using the 15% rise-time definition for the cases r = 2 (open circles) and r = 20 (x's). As in Fig. 7, the solid lines are computed using the Woodworth/Schlosberg formulas. Once again, these formulas provide a very good approximation.

## 6. CONCLUSIONS

Both theory and experiments show that the HRTF of a rigid sphere starts becoming sensitive to range when the ratio $\rho$ of the range to the radius is less than 5. The impulse response explains the source of the ripples in the frequency response, and provides direct information about the ITD. In particular, the ITD can be accurately computed by the generalized

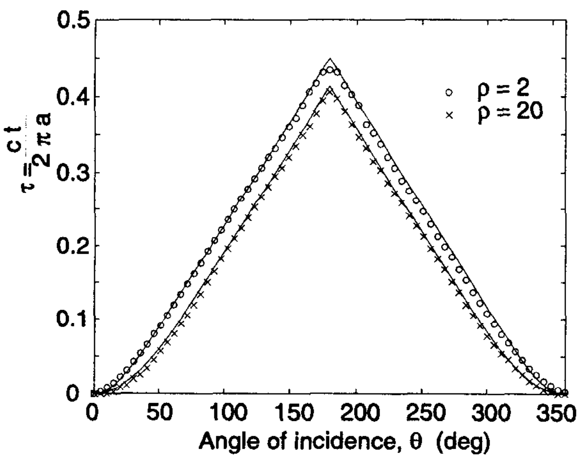


**Figure 11:** Measured arrival times compared to theory

Woodworth/Schlosberg formula, and is not very sensitive to range. By contrast, the ILD is very sensitive to range when the source is near, and becomes significant at quite low frequencies. Numerical analysis indicates that the HRTF is minimum phase. Thus, except for time delay, the impulse response can be reconstructed from a principle components analysis of the magnitude response.

## Acknowledgments

The material in this paper is based upon work supported by the National Science Foundation under Grant No. IRI-9402246. Any opinions, findings, and conclusions or recommendations expressed in this material are those of the authors and do not necessarily reflect the views of the National Science Foundation.

## REFERENCES

1. Brungart , D. S. and Rabinowitz, W. R. "Auditory localization in the near field," Third International Conference on Auditory Display, Palo Alto, CA (1996, unpublished).

2. Rabinowitz, W. M., Maxwell, J., Shao, Y., and Wei, M. "Sound localization cues for a magnified head: Implications from sound diffraction about a rigid sphere," *Presence* 2: 125-129 (1993).

3. Blauert, J., *Spatial Hearing* (revised edition) , MIT Press, Cambridge, MA, 1997.

4. Kuhn, G. F. "Model for the interaural time differences in the azimuthal plane," *J. Acoust. Soc. Am.* 62: 157-167, 1977.

5. Wiener, F. M. "Sound diffraction by rigid spheres and circular cylinders," *J. Acoust. Soc. Am.* 19: 444-451, 1947.